

An Assessment of ALE Mapping Technique for Buried Charge Simulations

İlker Kurtoğlu¹

¹FNSS Savunma Sistemleri A.Ş. – Turkey, Oğulbey Mah. Kumludere Caddesi No: 11 06830 Golbasi
Ankara

ilker.kurtoglu@fnss.com.tr

1 Abstract

In this work, the effects of ALE mapping technique developed by LSTC [1] are investigated for buried charge simulations. Before mapping studies, a mesh sensitivity study is performed for the pure ALE simulations to investigate the effect of 3D mesh size on the impulse. The ALE mapping is performed from a 2D axisymmetric model to full 3D model. The mapping time is decided by examining the pressure and velocity results of the 2D model simulations. The effect of different mesh ratios between the 2D and 3D model and the effect of 2D and 3D mesh sizes are also investigated. The impulse on the test plate is compared between all ALE models. Moreover, the normalized displacements at the center of the plates measured in the field tests are compared with the simulation results. A good correlation is obtained between the simulation and test results from the point of displacement.

Keywords: buried charge, ALE, mapping.

2 Introduction

Mine protection is a critical requirement for military vehicles. The vehicles should withstand the loads from the explosion and the secondary fragmentation. The mine protection level of the vehicles will depend on the customer needs or the standards defined by NATO [2]. The final validation of the vehicle against mine threat is performed by field tests. However, up to this point, computer simulations are used in every design stage. Therefore, the accuracy of the simulations should be reasonable in order to have a successful final design. For this reason, impulse on the structure due to the blast load should be predicted accurately and efficiently. In this work, the estimation of the impulse from the blast load is examined using pure ALE models and 2D to 3D ALE mapping.

Mapping technique is evaluated by Lapoujade et.al for air blast simulations [3]. They compared different mesh ratios and obtain peak overpressure with an error of less than 10% compared to the test results. Although the case in this study is different than the buried charge, it is taken as a baseline to start mapping studies for buried charges.

For the preprocessing of the keyword file LS-PrePost® 4.2 is used. For the preparation of mapping files, the SMP version of LS-DYNA® R7.1.1 (SVN 88920) and for the full 3D simulations, MPP version of LS-DYNA® R7.1.1 (SVN 88920) with Intel® MPI is used.

3 FE Model and Materials

The 3D model of the plate and the test setup is shown in Fig. 1 below. The setup is made of commercial steel and the test plate is made of RHA steel. There are 4 accelerometers installed on the plate and they are modeled with *ELEMENT_SEATBELT_ACCELEROMETER. Also, a deformation measurement cone which is made of very thin aluminum sheet is also utilized in the field tests to measure the total deformation in the plate. The deformation cone is not included in the simulations since it is designed such that it does not affect the total deformation of the test plate.

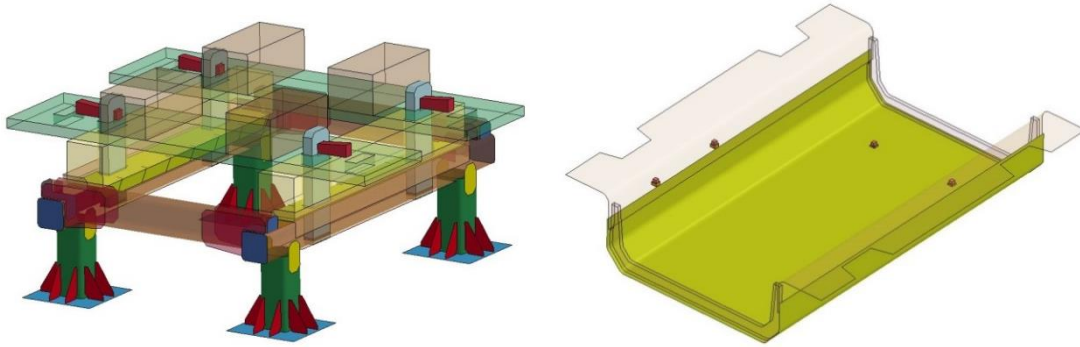


Fig. 1: Test setup (left) and the test plate assembly (right).

Three different ALE mesh is used in the full 3D simulations which are 20mm, 30mm and 40mm. For the mapping file generation model, a 2D axisymmetric model is used with 1mm, 2mm, 3mm and 4mm mesh sizes. The 2D and 3D ALE models are shown in Fig 2. The dimension of the 2D model is smaller than the 3D model as it can be seen from the dimensions.

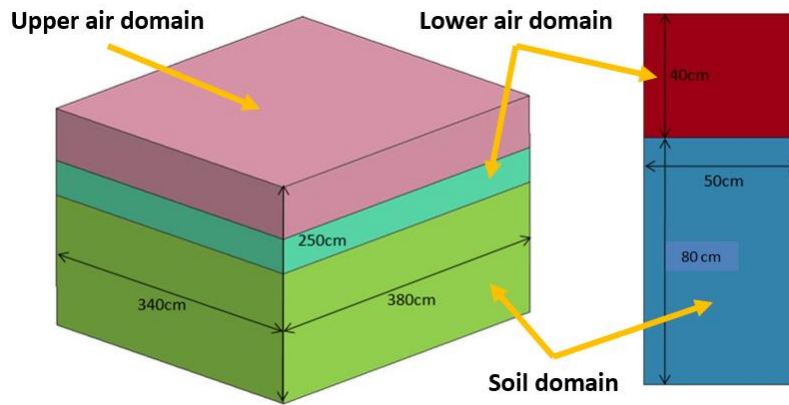


Fig. 2: Full 3D and axisymmetric 2D ALE models.

Air domain in the ALE model is divided into two parts, one of which is between the soil and the plate and the other one is the upside of the plate. Although single air domain is also applicable, this approach is selected to ensure more practical visualization and leakage optimization. The full 3D simulation model is shown in Fig 3.

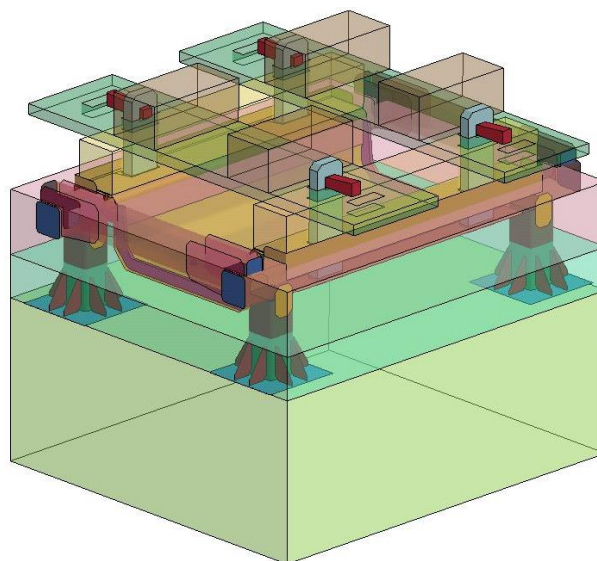


Fig. 3: Full 3D simulation model.

The air is modeled with `*MAT_NULL` and `*EOS_LINEAR_POLYNOMIAL`. The standard air parameters are used in the equation of state which is $C1=C2=C3=C6=0$, $C4=C5=0.4$, $E0=2.5e-6$ Mbars (so there is an initial pressure of 1 atmosphere in the air). By using `*LOAD_SEGMENT_SET` keyword, 1 atmosphere pressure is applied to the boundaries of the air in order not to let the air leak from the domain without any loading. The explosive material is modeled with `*MAT_HIGH_EXPLOSIVE_BURN` and `*EOS_JWL` equation of state with the parameters for TNT from [4]. The soil is modeled with `*MAT_SOIL_AND_FOAM_FAILURE` the parameters of which are determined in previous field tests. Test plate is modeled with `*MAT_SIMPLIFIED_JOHNSON_COOK`, the parameters of which are determined by Split-Hopkinson Pressure Bar tests in Izmir Institute of Technology. The ground is modeled with `*RIGIDWALL_PLANAR` by setting only the nodes of the lowest plates of the test setup as slave nodes to the rigid wall.

The interaction between the fluid parts (soil, lower air and explosive) and the plate is constructed with the `*CONSTRAINED_LAGRANGE_IN_SOLID` keyword. The parameters are optimized for each simulation to eliminate leakage. The air is divided into two different domains to visualize the leakage easier. The mapping process is done by `*INITIAL_ALE_MAPPING` keyword [5] along with the command line option "map=ale2d3d". The 3D simulations start where the 2D simulations end, in this case it is 400 micro seconds. All the simulations are done with `METH=-2` in the `*CONTROL_ALE` card.

4 Simulation Results and Discussion

4.1 Decision of Mapping Time

2D models are run for 2000 micro seconds in order to investigate the pressure and velocities at different heights from the ground. The aim is to stop the 2D simulation at a point where the pressure is the atmospheric pressure and velocities are zero just under the plate. For different mesh size comparison, pressure and velocity histories at different points are also investigated. The pressure and velocity histories at 20cm (T1), 30cm (T2) above the ground and just below the plate boundary (T3) for different mesh sizes are shown in Fig. 4 and 5 below.

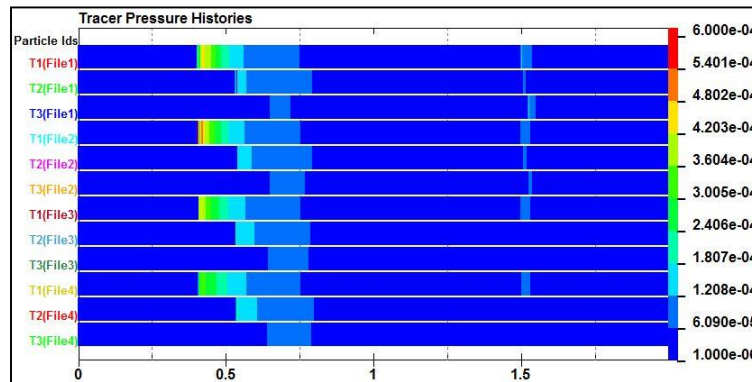


Fig.4: Pressure histories for the tracer points.

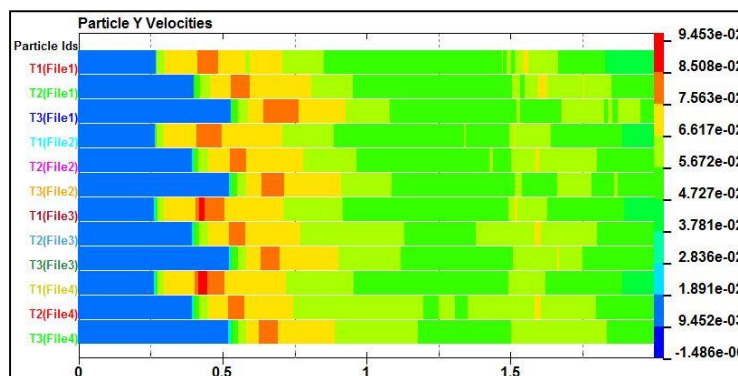


Fig.5: Y-Velocity histories for the tracer points.

When the figures are examined in detail, after 500 microseconds, the velocity starts to increase at the point placed just below the plate boundary. The mapping should be done before this time since the ALE-Lagrange coupling will become active after this step. For this study, 400 micro seconds is chosen as the 2D simulation time and 3D simulations will start after this point. The pressure distribution at 400 micro seconds in the 2D axisymmetric models are shown in Fig. 6 below.

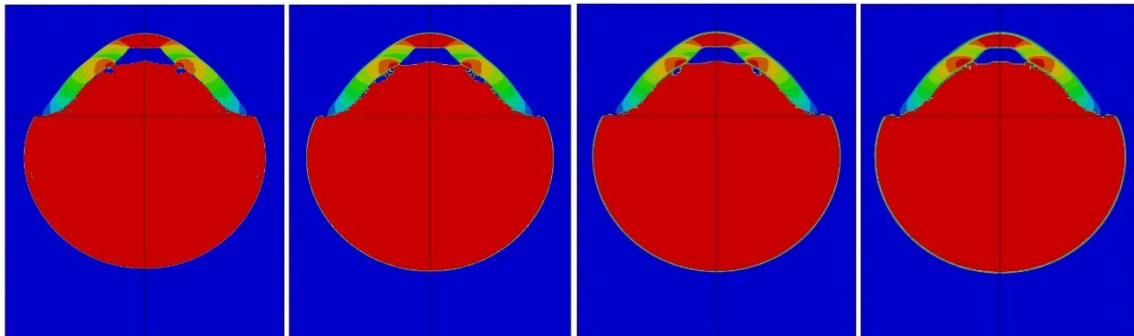


Fig.6: Pressure distributions for 2D models (1mm – 2mm – 3mm – 4mm).

It can be seen from Fig. 6 that the pressure waves do not reach to the boundaries of the 2D axisymmetric model which is also an important factor for deciding the mapping time and also the size of the 2D model.

4.2 Full 3D Model Simulations

At first, a comparison of the plate momentum is made for the pure ALE simulations. The momentum results without mapping are shown in Fig. 7 below.

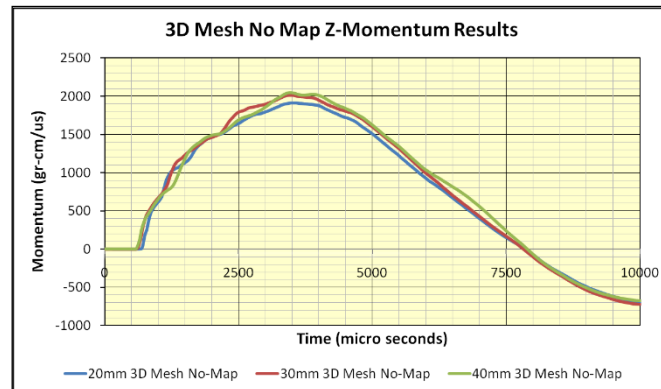


Fig.7: Z-Momentum results without mapping.

As it is seen in Fig. 7, the peak momentums obtained from different mesh sizes are different. The maximum momentum results are shown in Table 1.

	20mm Mesh	30mm Mesh	40mm Mesh
Momentum (gr-cm/μs)	1911.63	2010.04	2048.09

Table 1: Momentum results for 3D model without mapping.

The momentum results shows that as the mesh density is increasing, the Z-momentum on the plate is decreasing. Also, there are some differences in the time history of the momentum. This situation depends on the advection errors and the fluid structure interaction parameters for different mesh sizes. Moreover, the explosive material is filled with *INITIAL_VOLUME_FRACTION_GEOMETRY keyword into the ALE domain. Therefore the number of elements in the height of the explosive is different for each model which effects the advection of the explosive material and the soil. The simulation results at the point of peak momentum (~3450 μs) are shown for all 3D mesh models in the Fig. 8 below.

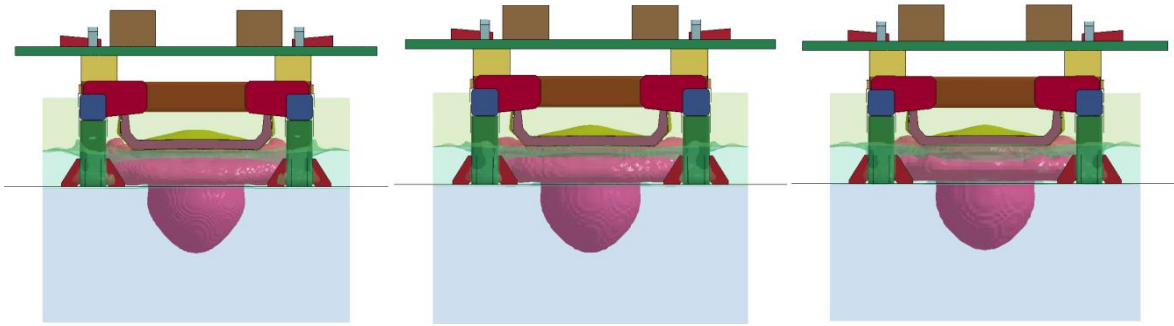


Fig.8: Simulation results of 3D models @3500 microseconds (20mm – 30mm – 40mm).

When Fig. 8 is examined, similar behaviors are observed with small differences. The soil behavior differs with the mesh size more remarkably. Moreover, in the sides of the bottom plate, there are some small differences in the advection of the explosive material. When mapping is used for 3D model with different mesh sizes, the obtained maximum values are shown in Table 2.

	3D Mesh Size	No Map	1mm Map	2mm Map	3mm Map	4mm Map
Momentum (gr-cm/μs)	20mm	1911.63	2100.83	2125.55	2151.00	2160.59
	30mm	2010.04	2111.96	2142.54	2115.95	2137.78
	40mm	2048.09	2119.34	2023.61	2054.68	2098.62

Table 2: 3D mapped results compared with no-map model.

It is observed that when 2D axisymmetric model is meshed with 1mm elements, the peak momentum results are very close to each other. When other mesh sizes are used in the 2D model, the momentum difference is more significant. This observation implies that the mapping results are closely related to the 2D model mesh size. If the 2D model is sufficiently fine to estimate the impulse, the results of the 3D models are nearly mesh independent. Not only the peak values but also the histories are examined in the Fig. 9, 10 and 11 below.

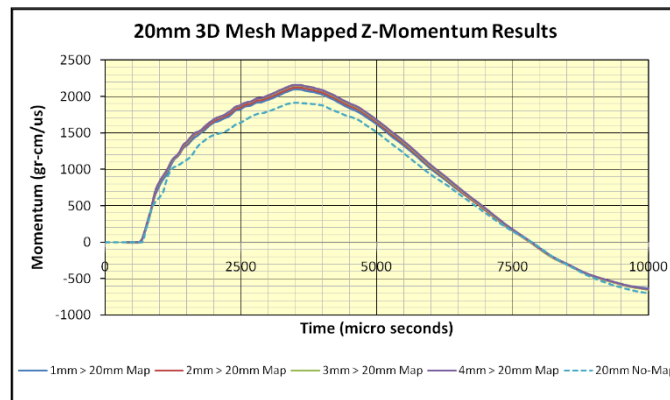


Fig.9: 20mm 3D mesh mapped results.

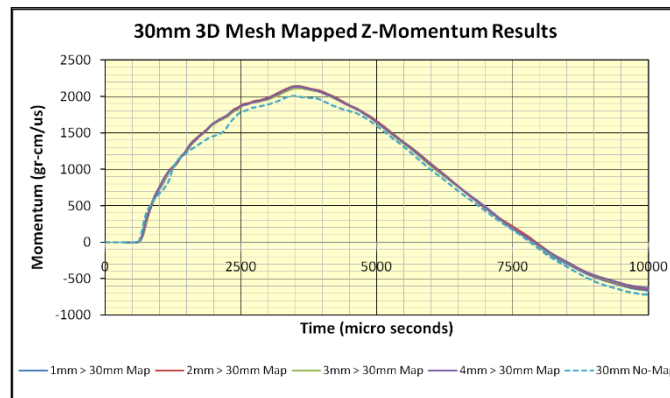


Fig.10: 30mm 3D mesh mapped results.

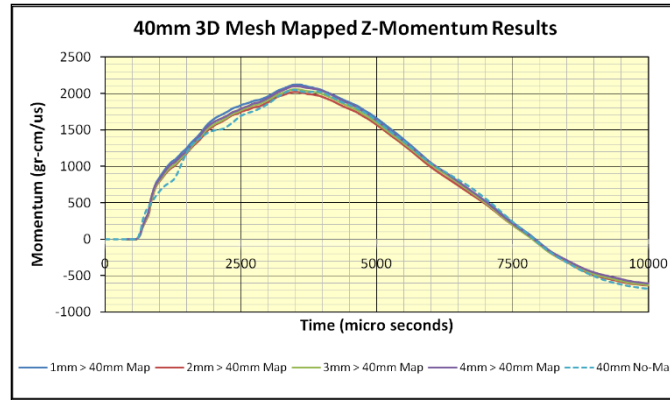


Fig. 11: 30mm 3D mesh mapped results.

The effect of mapping with different 2D mesh sizes is more significant in the results of 20mm and 30mm 3D mesh models. However, when the results in the Table 2 are examined, it will be noticed that the most effective results are obtained when the 2D mesh size is 1mm. The change in the momentum of the 1mm 2D mapped and no-map models with respect to the mesh size (1/h) is shown in Fig. 12.

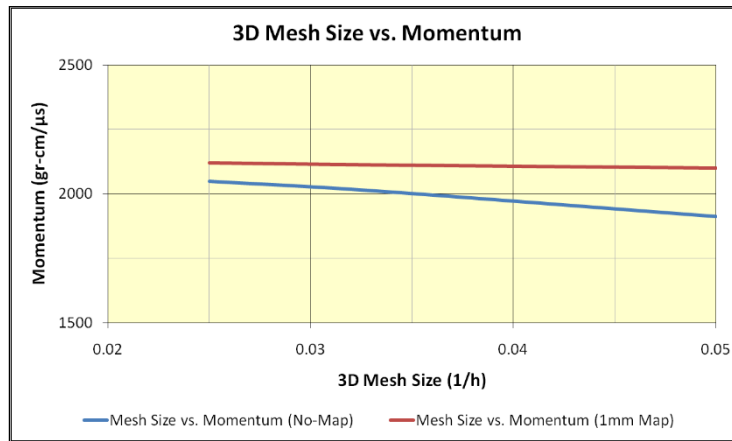


Fig. 12: Mesh size vs. momentum on the plate.

As it is said before, when the 2D mesh is fine enough, the 3D model results are nearly mesh independent. In Fig. 12, the mapped model results shows nearly a straight line behavior, however, the results of the model without mapping diverges from the maximum results when the element size is getting lower. Not only the peak values, but also the histories are also compared in Fig.13 below.

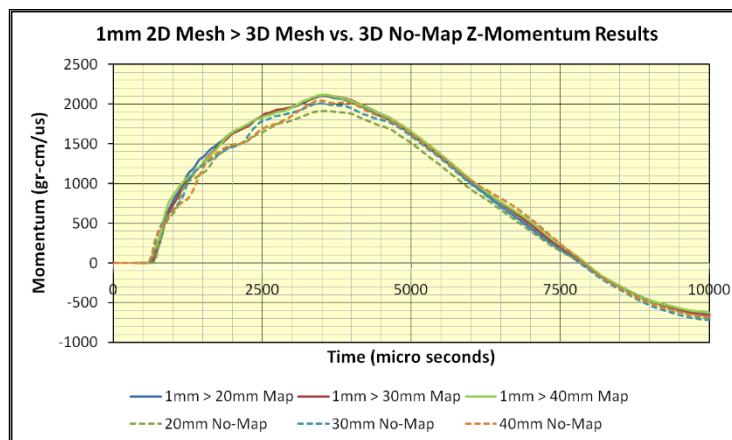


Fig. 13: 1mm map results compared to ones without mapping.

It can be seen that the histories of the mapped results of different 3D mesh sizes are similar. However, without mapping, the history is also affected from the mesh size. The behavior of the simulation at the peak momentum (~3450 μ s) is shown in the Fig. 14 below for 1mm map to the 3D models.

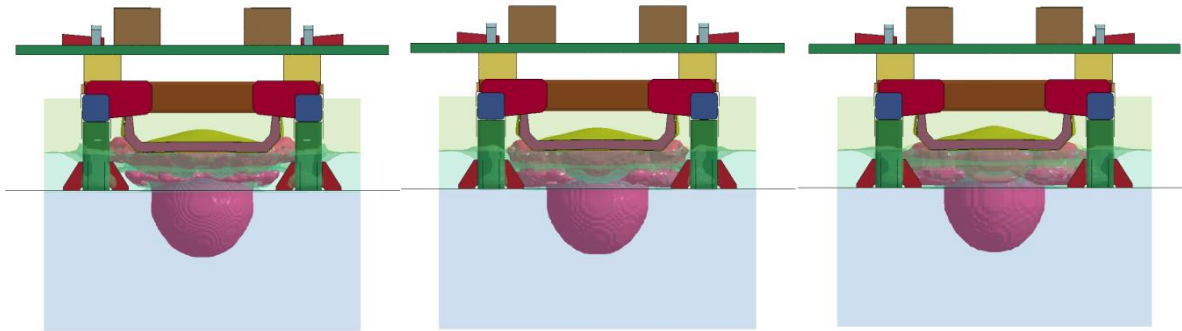


Fig. 14: Mapped simulation results @3500 microseconds (1mm map > 3D mesh)

When Fig 14 is examined in detail, there are still some differences as the ones obtained with no mapping 3D simulations. However, the momentum results are more consistent than the ones obtained in “no-mapping” 3D simulations.

The most important effect of this so-called mesh independency is in the solution time, which is compared for a 10,000 μ s simulation in Table 3 below.

Model	Total Simulation Time (s)
20mm No-Map	52967
30mm No-Map	15710
40mm No-Map	9557
1mm map → 20mm	47369
2mm map → 20mm	48792
3mm map → 20mm	54829
4mm map → 20mm	73176
1mm map → 30mm	15721
2mm map → 30mm	15884
3mm map → 30mm	16516
4mm map → 30mm	16246
1mm map → 40mm	9052
2mm map → 40mm	8563
3mm map → 40mm	8792
4mm map → 40mm	8989

Table 3: Total simulation time for models.

When the simulation times are compared between the same 3D mesh sizes, the 20mm mesh size model has an increasing solution time with increasing mesh size of the 2D axisymmetric model. However, the rest of the 3D models have similar solution times. When combined with the momentum effect, using 1mm 2D axisymmetric mesh with 40mm 3D mesh model will give the best solution time and optimum momentum estimation.

5 Normalized Displacement – Test vs. Simulation

The displacement results are compared with the test results in the Table 4 below. As stated before, for the measurement of total displacement, a deformation cone is used (made of very thin aluminum sheet) which is shown in the Fig. 15 below.



Fig. 15: Deformation cone used for total deformation measurement.

The difference between the initial and final length of the cone gives the total displacement of the midpoint of the plate. The design of the cone is performed with a considerable number of iterations to optimize the thickness of the cone in order not to affect the displacement of the test plate.

Model	Results	Model	Results	Model	Results
20mm	0.9195	30mm	0.9613	40mm	0.9789
1mm → 20mm	1.0148	1mm → 30mm	1.0094	1mm → 40mm	1.0685
2mm → 20mm	1.0365	2mm → 30mm	1.0085	2mm → 40mm	0.9962
3mm → 20mm	1.0407	3mm → 30mm	1.0088	3mm → 40mm	1.0013
4mm → 20mm	1.0434	4mm → 30mm	1.0220	4mm → 40mm	1.0126
TEST RESULT					1.0

Table 4: Normalized midpoint displacements

As it can be seen from Table 4, very close displacement results (less than $\pm 7\%$) are obtained with each model implying that small changes in the impulse does not affect the total displacement results significantly.

6 Summary and Future Work

In this work, the effects of ALE mapping technique on buried charge simulation results are investigated. The mapping is done from a 2D axisymmetric model to a 3D model up to 400 microseconds. The momentum results are fairly close when mapping is done from a 1mm 2D mesh to different 3D mesh sizes implying that for the impulse estimation high mesh ratios between 2D and 3D models can be used.

Acceleration data taken from various points shown in Fig. 1 are not validated. Acceleration history is important for the subcomponents installed on the bottom plate and sidewalls. Estimating the accelerations with reasonable accuracy will help the design of the mounting provisions of the subcomponents with simpler models. The validation study is still in progress.

The material model does not include any failure or damage model in this work. There is no failure observed in the test results, therefore modeling the damage and failure is not important for this study. However, there is always a possibility of failure especially in the welded joints of the hull plates and sub components. A project is started to characterize the failure and damage models of the base materials and welded joints. The results of this project will contribute to this study in the near future.

In this work, only METH=-2 is used in the *CONTROL_ALE keyword. For different advection methods, the effect is not investigated and is left for a future work.

7 Acknowledgments

This work is supported by Alper Tasdemirci (Izmir Institute of Technology) by means of determining the *MAT_SIMPLIFIED_JOHNSON_COOK material constants for RHA steel.

8 References

- [1] Aquelet N., Souli M., 2D to 3D ALE Mapping, 10th International LS-DYNA User's Conference, Detroit, USA, 2008.
- [2] AEP-55 Vol.2 Edition 2, Procedures for Evaluating the Protection Level of Armored Vehicles, 2010
- [3] Lapoujade V. (et. al), A Study of Mapping Technique for Air Blast Modeling, 11th International LS-DYNA® User's Conference, Detroit, USA, 2010.
- [4] Dobratz B. M., Crawford P. C., LLNL Explosives Handbook – Properties of Chemical Explosives and Explosive Stimulants, Lawrence Livermore National Laboratory, California, USA, 1985.
- [5] LS-DYNA Keyword manual R7.1.